発表者氏名	論文タイトル名	発表誌名	巻号	ページ	出版年
Takahashi Y, Tanaka R, Yamamoto N, Tanaka Y.	Enhancement of OX40-Induced Apoptosis by TNF Coactivation in OX40-Expressing T Cell Lines in Vitro Leading to Decreased Targets for HIV Type 1 Production.	AIDS Res Hum Retroviruses	24(3)	423-435	2008
Urano E, Shimizu S, Futahashi Y, Hamatake M, Morikawa Y, Takahashi N, Fukazawa H, Yamamoto N, Komano J.	Cyclin K/CPR4 inhibits primate lentiviral replication by inactivating Tat/positive transcription elongation factor b-dependent long terminal repeat transcription.	AIDS	22(9)	1081-1083	2008
Saito Y Yamamoto, N. Dewan Z, Sugimoto H, Martinez Bryun VJ, Iwasaki Y, Matsubara K, Qi X, Saitoh T, Imoto I, Inazawa I, Utsunomiya A, Watanabe T, Masuda T, Yamamoto N, Yamaoka S.	Overexpressed NF-kB inducing kinase contributes to the tumorigenesis of adult T-cell leukemia and Hodgkin Reed-Sternberg cells.	Blood	111(10)	5118-5129	2008
Ryo A, Tsurutani N, Ohba K, Kimura R, Komano J, Nishi M, Soeda H, Hattori S, Perrem K, Yamamoto M, Chiba J, Mimaya J, Yoshimura K, Matsushita S, Honda M, Yoshimura A, Sawasaki T, Aoki I, Morikawa Y, Yamamoto N.	SOCS1 is an inducible host factor during HIV-1 infection and regulates the intracellular trafficking and stability of HIV-1 Gag.	Proc Natl Acad Sci U S A	105(1)	294-299	2008
Okuma K, Tanaka R, Ogura T, Ito M, Kumakura S, Yanaka M, Nishizawa M, Sugiura W, Yamamoto N, Tanaka Y.	Interleukin-4-Transgenic hu-PBL-SCID Mice: A Model for the Screening of Antiviral Drugs and Immunotherapeutic Agents against X4 HIV-1 Viruses.	J Infect Dis	197(1)	134-141	2008
Miyakawa K, Ryo A, Murakami T, Ohba K, Yamaoka S, Fukuda M, Guatelli J, Yamamoto N.	BCA2/Rabring7 promotes tetherin-dependent HIV-1 restriction.	PLoS Pathog	5 (12)	e1000700	2009
Ohba K, Ryo A, Dewan MZ, Nishi M, Naito T, Qi X, Inagaki Y, Nagashima Y, Tanaka Y, Okamoto T, Terashima K, Yamamoto N.	Follicular dendritic cells activate HIV-1 replication in monocytes/macrophages through a juxtacrine mechanism mediated by P-selectin glycoprotein ligand 1.	J Immunol	183(1)	524-532	2009
Jeong SJ, Ryo A, Yamamoto N.	The prolyl isomerase Pin1 stabilizes the human T-cell leukemia virus type 1 (HTLV-1) Tax oncoprotein and promotes malignant transformation.	Biochem Biophys Res Commun	381(2)	294-299	2009

発表者氏名	論文タイトル名	発表誌名	巻号	ページ	出版年
Nishi M, Ryo A, Tsurutani N, Ohba K, Sawasaki T, Morishita R, Perrem K, Aoki I, Morikawa Y, Yamamoto N.	Requirement for microtubule integrity in the SOCS1-mediated intracellular dynamics of HIV-1 Gag.	FEBS Lett	583(8)	1243-1250	2009
Dewan MZ, Tomita M, Katano H, Yamamoto N, Ahmed S, Yamamoto M, Sata T, Mori N, Yamamoto N.	An HIV protease inhibitor, ritonavir targets the nuclear factor-kappaB and inhibits the tumor growth and infiltration of EBV-positive lymphoblastoid B cells.	Int J Cancer	124(3)	622-629	2009
梁　明秀					
Ryo A, Hirai A, Nishi M, Liou YC, Perrem K, Lin SC, Hirano H, Lee SW, Aoki I.	A suppressive role of the prolyl isomerase Pin1 in cellular apoptosis mediated by the death-associated protein Daxx.	J Biol Chem	282(50)	36671-36681	2007
Takeuchi R, Ryo A, Komitsu N, Mikuni-Takagaki Y, Fukui A, Takagi Y, Shiraishi T, Morishita S, Yamazaki Y, Kumagai K, Aoki I, Saito T.	Low-intensity pulsed ultrasound activates the phosphatidylinositol 3 kinase/Akt pathway and stimulates the growth of chondrocytes in three-dimensional cultures: a basic science study.	Arthritis Res Ther	10(4)	R77	2008
Masaoka T, Nishi M, Ryo A, Endo Y, Sawasaki T.	The wheat germ cell-free based screening of protein substrates of calcium/calmodulin-dependent protein kinase II delta.	FEBS Lett	582(13)	1795-1801	2008
Ryo A, Tsurutani N, Ohba K, Kimura R, Komano J, Nishi M, Soeda H, Hattori S, Perrem K, Yamamoto M, Chiba J, Mimaya J, Yoshimura K, Matsushita S, Honda M, Yoshimura A, Sawasaki T, Aoki I, Morikawa Y, Yamamoto N.	SOCS1 is an inducible host factor during HIV-1 infection and regulates the intracellular trafficking and stability of HIV-1 Gag.	Proc Natl Acad Sci U S A	105(1)	294-299	2008
Miyakawa K, Ryo A, Murakami T, Ohba K, Yamaoka S, Fukuda M, Guatelli J, Yamamoto N.	BCA2/Rabring7 promotes tetherin-dependent HIV-1 restriction.	PLoS Pathog	5(12)	e1000700	2009
Zhou W, Yang Q, Low CB, Karthik BC, Wang Y, Ryo A, Yao SQ, Yang D, Liou YC.	Pin1 catalyzes conformational changes of Thr-187 in p27Kip1 and mediates its stability through a polyubiquitination process.	J Biol Chem	284(36)	23980-23988	2009
Ohba K, Ryo A, Dewan MZ, Nishi M, Naito T, Qi X, Inagaki Y, Nagashima Y, Tanaka Y, Okamoto T, Terashima K, Yamamoto N.	Follicular dendritic cells activate HIV-1 replication in monocytes/macrophages through a juxtacrine mechanism mediated by P-selectin glycoprotein ligand 1.	J Immunol	183(1)	524-532	2009

発表者氏名	論文タイトル名	発表誌名	巻号	ページ	出版年
Jeong SJ, Ryo A, Yamamoto N.	The prolyl isomerase Pin1 stabilizes the human T-cell leukemia virus type 1 (HTLV-1) Tax oncoprotein and promotes malignant transformation.	Biochem Biophys Res Commun	381(2)	294-299	2009
Nishi M, Ryo A, Tsurutani N, Ohba K, Sawasaki T, Morishita R, Perrem K, Aoki I, Morikawa Y, Yamamoto N.	Requirement for microtubule integrity in the SOCS1-mediated intracellular dynamics of HIV-1 Gag.	FEBS Lett	583(8)	1243-1250	2009
Ryo A, Wulf G, Lee TH, Lu KP.	Pinning down HER2-ER crosstalk in SMRT regulation.	Trends Biochem Sci	34(4)	162-165	2009
Matsuura I, Chiang KN, Lai CY, He D, Wang G, Ramkumar R, Uchida T, Ryo A, Lu K, Liu F.	Pin1 promotes transforming growth factor-beta-induced migration and invasion.	J Biol Chem	285(3)	1754-1764	2010
澤崎達也					
Sawasaki T, Morishita R, Gouda MD, Endo Y.	Methods for high-throughput materialization of genetic information based on wheat germ cell-free expression system.	Methods Mol Biol	375	95-106	2007
Ryo A, Tsurutani N, Ohba K, Kimura R, Komano J, Nishi M, Soeda H, Hattori S, Perrem K, Yamamoto M, Chiba J, Mimaya J, Yoshimura K, Matsushita S, Honda M, Yoshimura A, Sawasaki T, Aoki I, Morikawa Y, Yamamoto N.	SOCS1 is an inducible host factor during HIV-1 infection and regulates the intracellular trafficking and stability of HIV-1 Gag.	Proc Natl Acad Sci U S A	105(1)	294-299	2008
Sawasaki T, Kamura N, Matsunaga S, Saeki M, Tsuchimochi M, Morishita R, Endo Y.	Arabidopsis HY5 protein functions as a DNA-binding tag for purification and functional immobilization of proteins on agarose/DNA microplate.	FEBS Lett	582(2)	221-228	2008
Tsuboi T, Takeo S, Iriko H, Jin L, Tsuchimochi M, Matsuda S, Han ET, Otsuki H, Kaneko O, Sattabongkot J, Udomsangpetch R, Sawasaki T, Torii M, Endo Y.	The Wheat germ cell-free based production of malaria proteins for discovery of novel vaccine candidates.	Infect Immun	76(4)	1702-1708	2008
Kobayashi T, Kodani Y, Nozawa A, Endo Y, Sawasaki T.	DNA-binding profiling of human hormone nuclear receptors via fluorescence correlation spectroscopy in a cell-free system.	FEBS Lett	582(18)	2737-2744	2008

発表者氏名	論文タイトル名	発表誌名	巻号	ページ	出版年
Masaoka T, Nishi M, Ryo A, Endo Y, Sawasaki T.	The wheat germ cell-free based screening of protein substrates of calcium/calmodulin-dependent protein kinase II delta.	FEBS Lett	582(13)	1795-1801	2008
Sawasaki T, Nishihara M, Endo Y.	RIP and RALyase cleave the sarcin/ricin domain, a critical domain for ribosome function, during senescence of wheat coleoptiles.	Biochem Biophys Res Commun	370(4)	561-565	2008
Bardóczy V, Géczi V Sawasaki T, Endo Y, Mészáros T.	A set of ligation-independent in vitro translation vectors for eukaryotic protein production.	BMC Biotechnol	8	32	2008
Shimada H, Hirai K, Simamura E, Hatta T, Iwakiri H, Mizuki K, Hatta T, Sawasaki T, Matsunaga S, Endo Y, Shimizu S.	Paraquat toxicity induced by voltage-dependent anion channel 1 acting as an NADH- dependent oxidoreductase.	J Biol Chem	284(42)	28642-28649	2009
Nozawa A, Matsubara Y, Tanaka Y, Takahashi H, Akagi T, Seki M, Shinozaki K, Endo Y, Sawasaki T.	Construction of a protein library of arabidopsis transcription factors using a wheat cell-free protein production system and its application for DNA binding analysis.	Biosci Biotechnol Biochem	73(7)	1661-1664	2009
Igawa T, Fujiwara M, Takahashi H, Sawasaki T, Endo Y, Seki M, Shinozaki K, Fukao Y, Yanagawa Y.	Isolation and identification of ubiquitin-related proteins from Arabidopsis seedlings.	J Exp Bot	60(11)	3067-3073	2009
Takahashi H, Nozawa A, Seki M, Shinozaki K, Endo Y, Sawasaki T.	A simple and high-sensitivity method for analysis of ubiquitination and polyubiquitination based on wheat cell-free protein synthesis.	BMC Plant Biology	9	39	2009
Takai K, Sawasaki T, Endo Y.	Practical cell-free protein synthesis system using purified wheat embryos.	Nature Protocols	5(2)	227-238	2010

III. 研究成果の刊行物・別刷（抜粋）

JOURNAL OF VIROLOGY, Dec. 2007, p. 13259–13264
0022-538X/07/$08.00+0 doi:10.1128/JVI.01353-07

Vol. 81, No. 23

Humanized NOD/SCID/IL2Rγ^{null} Mice Transplanted with Hematopoietic Stem Cells under Nonmyeloablative Conditions Show Prolonged Life Spans and Allow Detailed Analysis of Human Immunodeficiency Virus Type 1 Pathogenesis▽

Satoru Watanabe,[1,2] Shinrai Ohta,[3] Misako Yajima,[4] Kazuo Terashima,[5] Mamoru Ito,[6] Hideo Mugishima,[7] Shigeyoshi Fujiwara,[4] Kazufumi Shimizu,[2] Mitsuo Honda,[3] Norio Shimizu,[1]* and Naoki Yamamoto[3,5]*

Department of Virology, Division of Medical Science, Medical Research Institute, Tokyo Medical and Dental University, 1-5-45 Yushima, Bunkyo-ku, Tokyo 113-8519, Japan[1]; Open Research Center for Genome and Infectious Disease Control, Nihon University School of Medicine, 30-1 Oyaguchikami-chou, Itabashi-ku, Tokyo 173-8610, Japan[2]; AIDS Research Center, National Institute of Infectious Diseases, 1-23-1 Toyama, Shinjuku-ku, Tokyo 162-8640, Japan[3]; Department of Infectious Diseases, National Research Institute for Child Health and Development, 2-10-1 Okura, Setagaya-ku, Tokyo 154-8567, Japan[4]; Department of Molecular Virology, Graduate School of Medicine, Tokyo Medical and Dental University, 1-5-45 Yushima, Bunkyo-ku, Tokyo 113-8519, Japan[5]; Central Institute for Experimental Animals, 1430 Nogawa, Miyamae-ku, Kawasaki, Kanagawa 216-0001, Japan[6]; and Department of Pediatrics and Child Health, Nihon University School of Medicine, 30-1 Oyaguchikami-chou, Itabashi-ku, Tokyo 173-8610, Japan[7]

Received 21 June 2007/Accepted 3 September 2007

In a previous study, we demonstrated that humanized NOD/SCID/IL2Rγ^{null} (hNOG) mice constructed with human hematopoietic stem cells (HSCs) allow efficient human immunodeficiency virus type 1 (HIV-1) infection. However, HIV-1 infection could be monitored for only 43 days in the animals due to their short life spans. By transplanting HSCs without any myeloablation methods, the mice successfully survived longer than 300 days with stable engraftment of human cells. The mice showed high viremia state for more than the 3 months examined, with systemic HIV-1 infection and gradual decrease of CD4$^+$ T cells analogous to that in humans. These capacities of the hNOG mice are very attractive for modeling mechanisms of AIDS progression and therapeutic strategy.

One of the main problems in the field of human immunodeficiency virus type 1 (HIV-1) research is the lack of suitable small animal models for studying the virological and pathogenic aspects of human HIV-1 infection. To overcome the drawback that HIV-1 does not replicate in rodent cells, severe combined immunodeficiency (SCID) mice, engrafted with human peripheral blood mononuclear cells (hu-PBL-SCID) (16) or human fetal thymus and liver tissue [SCID-hu (Thy/Liv)] (18), have been used for the small animal models of HIV-1 infection. However, these mouse models fall short of accurately mirroring human HIV infection because of their short infection spans (17), limited infection of lymphoid tissues (15), and partial infection to coreceptor tropic HIVs (4, 10, 13).

Considering the significant advantages of developing a mouse model for HIV-1 infection, we previously introduced a novel HIV-1 mouse model using nonobese diabetic (NOD)/SCID/interleukin-2 receptor (IL-2R) gamma chain-knocked-out (NOG) mice (22). Multilineage human cells, including T, B, NK cells, monocytes/macrophages, and dendritic cells (DCs) differentiate in the mice when transplanted with human CD34$^+$ hematopoietic stem cells (HSCs) (6, 9, 22). These mice show high levels of susceptibility to both CCR5 (R5)- and CXCR4 (X4)-tropic HIVs with intense plasma viral loads lasting for over 40 days (22). Thus, this mouse model may be valuable for the study of HIV-1 infection. However, a serious problem remains. The mice showed symptoms of a wasting condition and a hunched back 5 to 7 months after HSC transplantation, following which most of them died. This life span is not sufficient if we are to better understand HIV pathogenesis and to develop novel anti-HIV countermeasures, because more than 4 months posttransplantation is required for the development of human T cells before HIV-1 can be studied in mice.

In past studies for the construction of humanized mouse models using NOD/SCID, β2 microglobulin-deficient NOD/SCID (NOD/SCID/B2m^{null}) or NOG mice, the mice were subjected to total body irradiation or given drugs for HSC transplantation (6, 9, 11, 14, 21, 23). Since NOG mice do not develop any thymic lymphomas in contrast to NOD/SCID or NOD/SCID/B2m^{null} mice (3, 19), the irradiation might influence the reduction of their life spans. In this study, we therefore searched for optimal conditions for HSC transplantation and consequently found that in NOG mice, myeloablation procedures were not required for human cell generation. Importantly, these mice stably survived

* Corresponding author. Mailing address for Naoki Yamamoto: AIDS Research Center, National Institute of Infectious Diseases, 1-23-1 Toyama, Shinjuku-ku, Tokyo 162-8640, Japan. Phone: 81-3-5285-1111. Fax: 81-3-5285-1165. E-mail: nyama@nih.go.jp. Mailing address for Norio Shimizu: Department of Virology, Division of Medical Science, Medical Research Institute, Tokyo Medical and Dental University, 1-5-45 Yushima, Bunkyo-ku, Tokyo 113-8519, Japan. Phone and fax: 81-3-5803-5811. E-mail: nshivir@tmd.ac.jp.

▽ Published ahead of print on 19 September 2007.

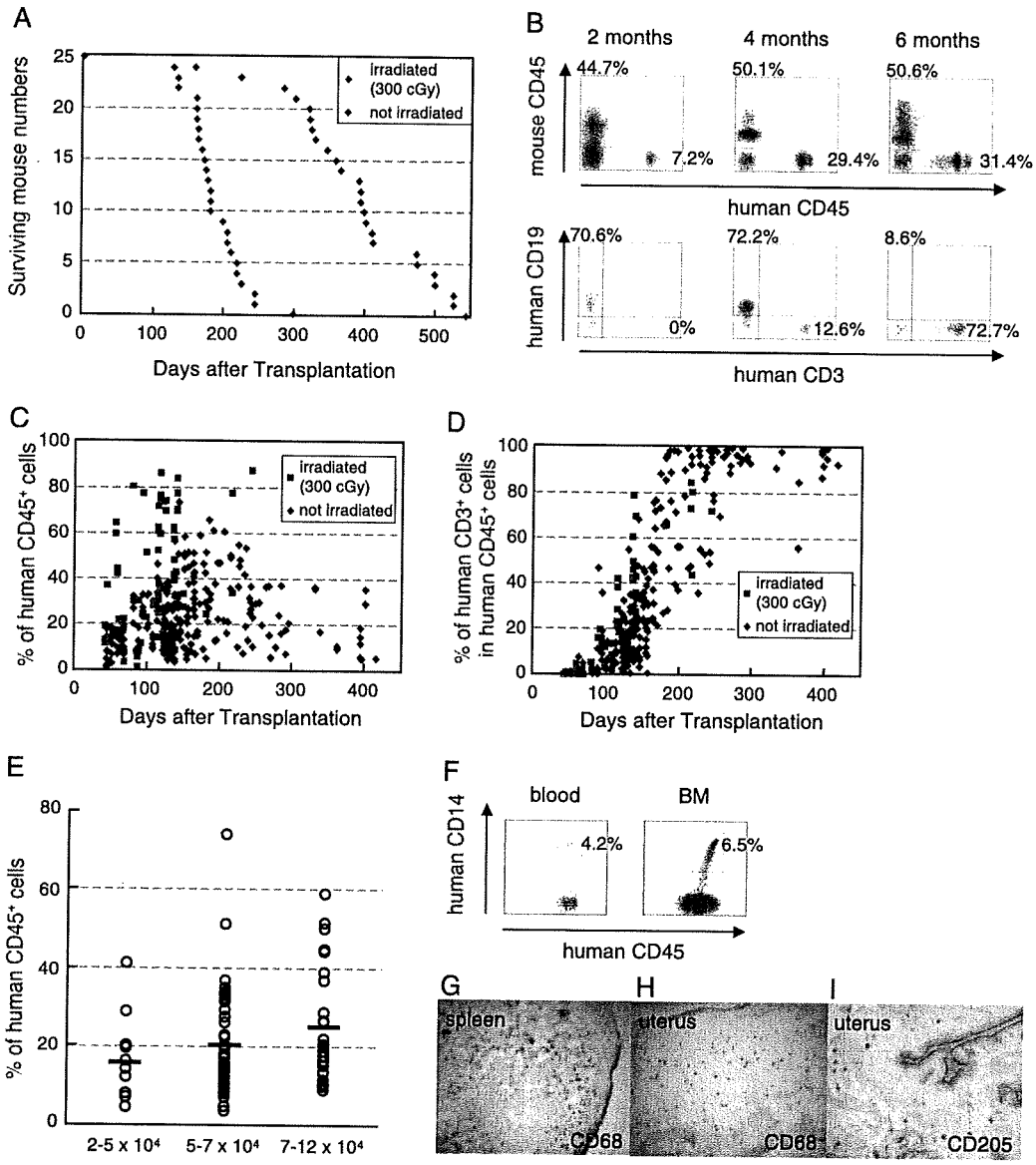

FIG. 1. Human cell generation in hematopoietic stem cell-engrafted hNOG mice with or without myeloablation. (A) Life spans of NOG mice transplanted with human stem cells after receiving 300 cGy irradiation (n = 25) or not receiving irradiation (n = 25). (B) Representative flow cytometric profiles of the mice from 2 to 6 months after transplantation without irradiation. The ratio of human to murine $CD45^+$ cells and that of human $CD3^+$ cells to $CD19^+$ cells are shown. Note that the mice generated human $CD45^+$ leukocytes that eventually developed human $CD19^+$ B cells first and then $CD3^+$ T cells. (C and D) Percentages of human $CD45^+$ cells (C) and $CD3^+$ T cells in human $CD45^+$ cells (D) in peripheral blood from 65 mice that received 300 cGy irradiation and 222 nonirradiated mice 40 to 413 days after transplantation. (E) Summary of engraftment levels in nonirradiated mice transplanted with 2×10^4 to 5×10^4 cells (n = 11), 5×10^4 to 7×10^4 cells (n = 53), or 7×10^4 to 12×10^4 (n = 30) human stem cells. Percentages of human $CD45^+$ leukocytes in peripheral blood during 4 to 5 months after transplantation were shown. The horizontal black bars indicate the averages of the groups. (F to I) Flow cytometric analysis and immunohistochemical analysis of the expression of myelomonocytic markers in nonirradiated mice 4 months after transplantation. Human $CD14^+$ monocytes/macrophages were recognized in peripheral blood and BM (F). A gate was set on the human $CD45^+$ population. Human $CD68^+$ macrophages and $CD205^+$ DCs were also detected in spleen (G) and uterus (H and I). Visualization was performed with 5-bromo-4-chloro-3-indolylphosphate (BCIP). The original magnifications were ×100 (G and H) and ×200 (I).

longer than 300 days after the HSC transplantation, which allowed further investigation of HIV-1 pathogenesis and progression to disease state in the animals.

NOG mice constructed with HSCs without myeloablation showed prolonged survival time and stable human cell generation. Six- to eight-week-old female NOG mice were obtained from the Central Institute for Experimental Animals (Kawasaki, Japan), and human cord blood-derived $CD34^+$ HSCs (2×10^4 to 12×10^4 cells) were injected intravenously with or without irradiation. As shown in Fig. 1A, most of the mice that received 300 cGy irradiation were dead within 250 days post-transplantation (mean survival time, 188 days). In contrast, more than 80% of the mice with transplanted HSCs without irradiation survived over 300 days (mean survival time, 387

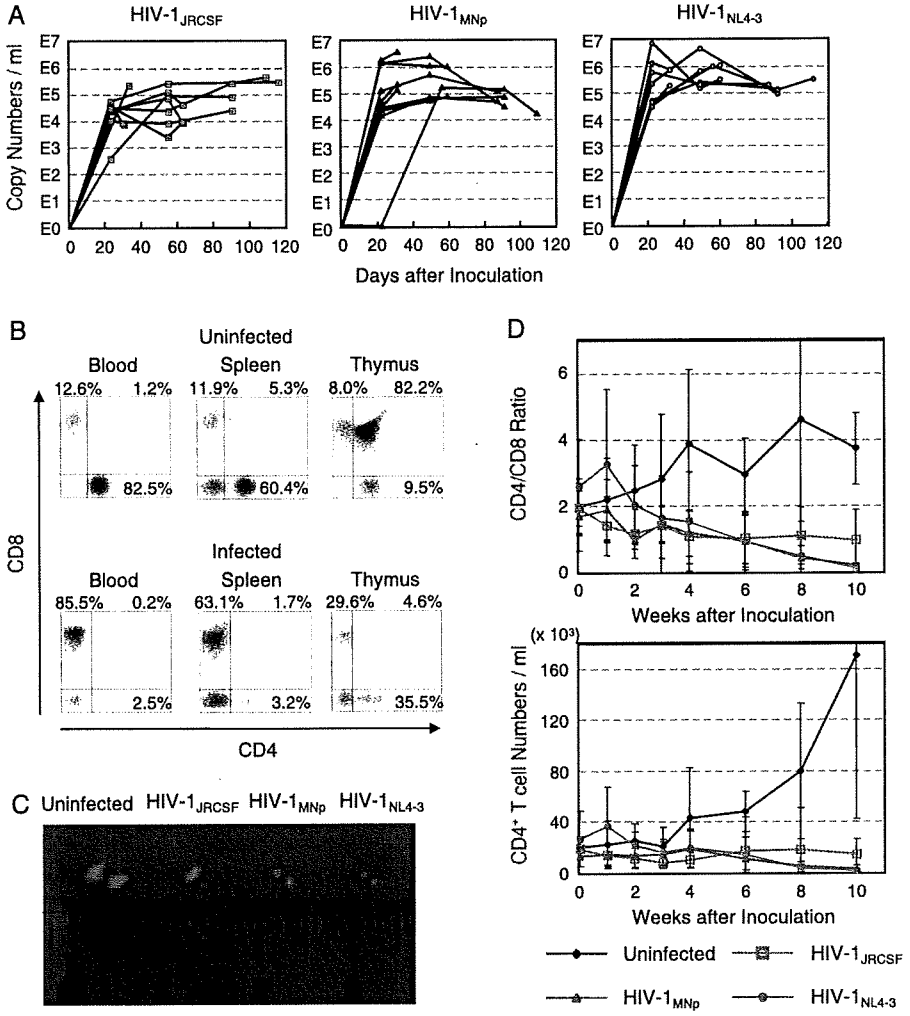

FIG. 2. Long-lasting viremia and $CD4^+$ T-cell depletion in R5- and X4-tropic HIV-1-infected hNOG mice. (A) Viral copy numbers in plasma from 29 mice intravenously inoculated with R5-tropic $HIV\text{-}1_{JRCSF}$ (65,000 $TCID_{50}$; $n = 11$), X4-tropic $HIV\text{-}1_{MNp}$ (20,000 $TCID_{50}$; $n = 10$), and X4-tropic $HIV\text{-}1_{NL4\text{-}3}$ (60,000 $TCID_{50}$; $n = 8$). RNA viral copy numbers were measured using a real-time PCR quantification assay as previously described (22). (B) The percentages of $CD4^-$ $CD8^+$ (top left), $CD4^+$ $CD8^+$ (top right), and $CD4^+$ $CD8^-$ (bottom right) cells in blood, spleen, and thymus from a uninfected control mouse and a $V\text{-}1_{NL4\text{-}3}$-infected mouse (32 days postinfection). These two mice were constructed with HSCs from the same cord blood donor, and sacrificed 181 and 169 days after transplantation, respectively. A gate was set on the human $CD45^+$ population. (C) Comparison of the apparent size of mesenteric LN from uninfected mice or mice infected with $HIV\text{-}1_{JRCSF}$ (109 days postinfection), $HIV\text{-}1_{MNp}$ (109 days postinfection), or $HIV\text{-}1_{NL4\text{-}3}$ (112 days postinfection). A uninfected control mouse was sacrificed 249 days after transplantation, and three HIV-1-infected mice were sacrificed 246, 246, and 249 days after transplantation. (D) Comparison of CD4/CD8 T-cell ratios and absolute $CD4^+$ T-cell numbers in peripheral blood from uninfected control mice ($n = 7$), R5-tropic $HIV\text{-}1_{JRCSF}$-infected mice ($n = 7$), X4-tropic $HIV\text{-}1_{MNp}$-infected mice ($n = 5$), and X4-tropic $HIV\text{-}1_{NL4\text{-}3}$-infected mice ($n = 6$). Results are expressed as means ± standard deviations (error bars).

days). These mice were successfully engrafted with HSCs, resulting first in the generation of human $CD19^+$ B cells and subsequently in the generation of human $CD3^+$ T cells (Fig. 1B). Figure 1C and D show the percentages of human $CD45^+$ leukocytes and human $CD3^+$ T cells in peripheral blood at 40 to 413 days after HSC transplantation. Up to 74% of leukocytes in peripheral blood samples were reconstituted with human cells in nonirradiated mice (mean ± standard deviation, 22.8% ± 14.0%; $n = 222$), and this was maintained over 400 days after transplantation (Fig. 1C). Although higher levels of human cell reconstitution were observed in the irradiated mice (45.2% ± 23.9%; $n = 65$) (Fig. 1C), which may be due to reduction of absolute numbers of murine cells by destruction of their progenitor cells in bone marrow (BM), human $CD3^+$ T cells developed with similar kinetics between the two groups (Fig. 1D). Figure 1E shows the engraftment efficiency of NOG mice transplanted with different numbers of HSCs without irradiation. More than 2×10^4 HSCs could be stably engrafted, and the levels of human cell reconstitution increased relative to the number of transplanted cells.

We further analyzed the development of human monocytes, macrophages, and DCs in the mice with transplanted HSCs without irradiation. Human $CD14^+$ monocytes were detected in peripheral blood and BM using flow cytometry (Fig. 1F), and many human $CD68^+$ macrophages were observed in various organs, including spleen (Fig. 1G), uterus (Fig. 1H), ovary, and lung (data not shown). Human $CD205^+$ DCs were also detected in spleen (data not shown) and uterus (Fig. 1I). These

TABLE 1. CD4/CD8 ratios in peripheral blood and spleen and $CD4^+$ $CD8^+$ cells in thymus of groups of uninfected and HIV-1-infected mice[a]

Group and mouse identification no.	No. of days after inoculation	CD4/CD8 ratio		% of $CD4^+$ $CD8^+$ cells in thymus	No. of RNA viral copies/ml
		Blood	Spleen		
Uninfected control group (n = 15)		2.92 ± 1.68	2.78 ± 1.46	67.8 ± 20.5	
$HIV\text{-}1_{JRCSF}$-infected group					
1	30	1.86	0.88	77.1	9,078
2	30	0.46	0.53	12.5	7,703
3	33	2.61	2.17	85.7	223,020
4	63	0.17	0.27	25.5	9,965
5	63	0.36	0.44	27.2	8,734
6	63	0.18	0.88	69.6	42,198
7	90	0.03	0.37	82.5	24,441
8	90	0.30	0.79	84.6	24,454
9	90	1.77	1.55	56.9	80,636
10	109	0.20	0.17	43.4	470,392
11	116	0.09	0.78	11.8	299,080
$HIV\text{-}1_{MNp}$-infected group					
1	31	0.82	0.44	34.6	3,709,520
2	31	1.02	0.61	90.2	219,971
3	31	1.64	1.57	78.2	135,592
4	59	0.21	0.38	35.4	78,848
5	59	0.10	0.07	77.0	1,039,716
6	87	0.20	0.40	0.5	49,080
7	87	0.19	0.08	11.7	121,817
8	91	0.04	0.04	82.9	30,706
9	91	0.28	0.10	1.2	7,407
10	109	0.00	0.21	2.8	17,310
$HIV\text{-}1_{NL4\text{-}3}$-infected group					
1	32	1.01	0.81	64.5	195,375
2	32	0.03	0.05	4.6	770,721
3	60	0.21	0.13	3.9	1,108,003
4	60	0.14	ND[b]	ND	328,375
5	87	0.03	0.04	1.0	201,207
6	92	0.03	0.17	11.1	90,831
7	92	0.03	0.03	1.4	135,514
8	112	0.30	0.23	0.2	325,202

[a] Twenty-nine mice inoculated with R5-tropic $HIV\text{-}1_{JRCSF}$ (n = 11), X4-tropic $HIV\text{-}1_{MNp}$ (n = 10), or X4-tropic $HIV\text{-}1_{NL4\text{-}3}$ (n = 8) were sacrificed 161 to 249 days after HSC transplantation. Fifteen uninfected control mice were sacrificed 174 to 249 days after transplantation, and results for the control group are expressed as means ± standard deviations.

[b] ND, not determined because of a lack of cells.

observations were similar to those seen in irradiated mice as shown in our previous report (22). Thus, humanized NOG (hNOG) mice without any myeloablation procedures allowed sufficient development of human cells to study HIV-1 pathogenesis.

hNOG mice induced systemic and long-lasting HIV-1 infection with $CD4^+$ T-cell depletion. We prepared 29 stem cell-transplanted hNOG mice and inoculated them intravenously with a high dose of R5-tropic $HIV\text{-}1_{JRCSF}$ (65,000 50% tissue culture infective doses [$TCID_{50}$]), X4-tropic $HIV\text{-}1_{MNp}$ (20,000 $TCID_{50}$), or X4-tropic $HIV\text{-}1_{NL4\text{-}3}$ (60,000 $TCID_{50}$) at 122 to 150 days posttransplantation. Then, plasma viral RNA copy numbers were measured at successive time points. The mice showed marked, long-lasting viremia state for more than 3 months, reaching the highest levels of 3.0×10^5 copies/ml from $HIV\text{-}1_{JRCSF}$-infected mice, 3.7×10^6 copies/ml from $HIV\text{-}1_{MNp}$-infected mice, and 7.8×10^6 copies/ml from $HIV\text{-}1_{NL4\text{-}3}$-infected mice (Fig. 2A). None of the mice weakened or died as a result of HIV-1 infection throughout the entire follow-up period.

All the mice were sacrificed within 4 months postinfection, and the percentages of $CD4^+$ and $CD8^+$ cells in lymphoid tissues were analyzed by flow cytometry. In a representative HIV-1-infected mouse, as shown in Fig. 2B, CD4/CD8 ratios in blood and spleen significantly decreased with apparent loss of $CD4^+$ $CD8^+$ double positive thymocytes. The size of lymphoid tissues, such as thymus and lymph node (LN), in the HIV-1-infected mice was very small compared with uninfected mice (Fig. 2C), suggesting that they shrank as a result of HIV-1 infection. Table 1 illustrates the overall profile of CD4/CD8 ratios in blood and spleen and the percentages of $CD4^+$ $CD8^+$ thymocytes from the 29 HIV-1-infected mice. Most of the mice, both R5- and X4-tropic and HIV-1 infected, had reduced CD4/CD8 ratios in blood and spleen compared with unin-

TABLE 2. Comparison of DNA proviral copies in various organs from HIV-1-infected mice[a]

Organ	No. of HIV-1 DNA copies/100 ng DNA in mice infected with[b]:		
	HIV-1_{JRCSF}	HIV-1_{MNp}	HIV-1_{NL4-3}
Peripheral blood	60	6	UD
Spleen	793	1,143	2,115
Bone marrow	2,432	656	584
Thymus	23	2,074	17,374
Lymph node	2,103	942	2,115
Lung	239	145	177
Liver	74	49	12
Small intestine	ND	6	9
Ovary	24	122	10
Uterus	14	5	16
Rectum	UD	16	11
Heart	9	UD	UD
Skin	UD	UD	138
Brain	UD	2	UD
Eyeball	3	25	UD

[a] Viral DNA was extracted from various organs of mice infected with HIV-1_{JRCSF} (33 days postinfection), HIV-1_{MNp} (59 days postinfection), and HIV-1_{NL4-3} (60 days postinfection). Determination of HIV-1 DNA copy numbers was performed by real-time PCR assay as previously described (22).

[b] UD, undetected; ND, not done.

fected control mice. On the other hand, a reduction of $CD4^+$ $CD8^+$ thymocytes was observed especially in X4-tropic HIV-1-infected mice, which seemed to correlate with the predominant expression of CXCR4 on the thymocytes as we previously described (22). Interestingly, two mice that were infected with HIV-1_{MNp} (mouse identification number 5 and 8) maintained their high percentages of $CD4^+$ $CD8^+$ thymocytes in spite of significant CD4/CD8 decline in their blood and spleen, suggesting no direct relationship between thymic T-cell depletion and CD4/CD8 decrease in peripheral blood or spleen by HIV-1 infection.

In one mouse from each R5- and X4-tropic HIV-infected group, HIV-1 proviral DNA copy numbers in various organs were measured by real-time PCR assay (Table 2). High HIV DNA copy numbers were detected in the spleen, BM, and LN of the R5-tropic HIV-1-infected mouse and in the thymus, spleen, and LN of the X4-tropic HIV-1-infected mice. In addition, HIV DNA copies were detectable in various other organs, including the lung, liver, ovary, and uterus. The fact that many human $CD68^+$ macrophages, the source of HIV-1 throughout the body (7, 8), were recognized in these organs (22) (Fig. 1H) may help explain the susceptibility of these organs to HIV-1.

To further investigate the progression of $CD4^+$ T-cell depletion by HIV-1 infection, 25 mice 120 to 151 days after HSC transplantation were randomly separated into groups of uninfected control mice ($n = 7$), HIV-1_{JRCSF}-inoculated mice ($n = 7$), HIV-1_{MNp}-inoculated mice ($n = 5$), and HIV-1_{NL4-3}-inoculated mice ($n = 6$), and then CD4/CD8 ratios and absolute $CD4^+$ T-cell numbers in peripheral blood were monitored at regular intervals. X4-tropic HIV-infected mice showed gradual decreases of their CD4/CD8 ratios and $CD4^+$ T-cell numbers, which eventually resulted in an almost complete depletion from peripheral blood (Fig. 2D). While $CD4^+$ T-cell depletion was also seen in R5-tropic HIV-infected mice, this was less prominent compared with X4-tropic HIV-1-infected mice (Fig. 2D). This pattern of R5- versus X4-tropic HIV-1 infection seems to correlate with the general observation that the emergence of X4-tropic HIVs accelerates $CD4^+$ T-cell decline and disease progression in HIV patients (12, 20).

In this study, we successfully prolonged the life span of hNOG mice by improving the HSC transplantation method and further clarified characteristics of HIV-1 infection in the mice including the following: (i) high levels of viremia lasting over 3 months, (ii) $CD4^+$ T-cell depletion in peripheral blood and spleen regardless of thymic T-cell loss, (iii) systemic HIV-1 infection not only in lymphoid tissues but also in various other organs, and (iv) a different rate of $CD4^+$ T-cell depletion for R5- versus X4-tropic HIV-1 strains. Recently, several studies on HIV-1 infection in $Rag2^{-/-}$ $\gamma c^{-/-}$ mice, transplanted with HSCs at birth, have also been reported (1, 2, 5, 24). The mice showed high susceptibility to both R5- and X4-tropic HIVs and long-term viremia with $CD4^+$ T-cell depletion, which is partly similar to our present results. However, the efficiency of human cell generation in $Rag2^{-/-}$ $\gamma c^{-/-}$ mice strongly depends on the dose of irradiation, and levels of chimerism in mice are not stable even receiving 550 to 750 cGy irradiation, which does eventually induces reduction of their life spans (5). In contrast, very stable engraftment of HSCs and subsequent human cell generation were noted in our hNOG mice even without any myeloablation procedures. Their long life spans and long-term human cell reconstitution allowed persistent HIV-1 infections mirroring HIV-1 infections in humans. Thus, this hNOG mouse system is a very useful tool as an advanced mouse model for the study of AIDS progression and long-term evaluation of new anti-HIV-1 drugs.

We thank Tomohiro Morio, Ken Watanabe, and Eiko Ogata of Tokyo Medical and Dental University for their helpful comments and skillful technical support. We are also grateful to Yukari Sasaki and Kazuhiro Takimoto of the National Institute of Infectious Diseases and Teruaki Tanaka and Junichi Fujita of the Nihon University School of Medicine for their management of animals. Human umbilical cord blood samples were obtained from the Tokyo Cord Blood Bank of the Nihon University School of Medicine.

This work was supported by a grant from the Ministry of Education, Culture, Sports, Science, and Technology to promote open research for young academics and specialists.

REFERENCES

1. **Baenziger, S., R. Tussiwand, E. Schlaepfer, L. Mazzucchelli, M. Heikenwalder, M. O. Kurrer, S. Behnke, J. Frey, A. Oxenius, H. Joller, A. Aguzzi, M. G. Manz, and R. F. Speck.** 2006. Disseminated and sustained HIV infection in $CD34^+$ cord blood cell-transplanted $Rag2^{-/-}$ $\gamma c^{-/-}$ mice. Proc. Natl. Acad. Sci. USA **103**:15951–15956.
2. **Berges, B. K., W. H. Wheat, B. E. Palmer, E. Connick, and R. Akkina.** 2006. HIV-1 infection and CD4 T cell depletion in the humanized $Rag2^{-/-}$ $\gamma c^{-/-}$ (RAG-hu) mouse model. Retrovirology **3**:76.
3. **Christianson, S. W., D. L. Greiner, R. A. Hesselton, J. H. Leif, E. J. Wagar, I. B. Schweitzer, T. V. Rajan, B. Gott, D. C. Roopenian, and L. D. Shultz.** 1997. Enhanced human $CD4^+$ T cell engraftment in beta2-microglobulin-deficient NOD-scid mice. J. Immunol. **158**:3578–3586.
4. **Fais, S., C. Lapenta, S. M. Santini, M. Spada, S. Parlato, M. Logozzi, P. Rizza, and F. Belardelli.** 1999. Human immunodeficiency virus type 1 strains R5 and X4 induce different pathogenic effects in hu-PBL-SCID mice, depending on the state of activation/differentiation of human target cells at the time of primary infection. J. Virol. **73**:6453–6459.
5. **Gorantla, S., H. Sneller, L. Walters, J. G. Sharp, S. J. Pirruccello, J. T. West, C. Wood, S. Dewhurst, H. E. Gendelman, and L. Poluektova.** 2007. Human immunodeficiency virus type 1 pathobiology studied in humanized BALB/c-$Rag2^{-/-}\gamma_c^{-/-}$ mice. J. Virol. **81**:2700–2712.
6. **Hiramatsu, H., R. Nishikomori, T. Heike, M. Ito, K. Kobayashi, K. Katamura, and T. Nakahata.** 2003. Complete reconstitution of human lym-

phocytes from cord blood CD34$^+$ cells using the NOD/SCID/γ_c^{null} mice model. Blood **102:**873–880.

7. **Igarashi, T., C. R. Brown, Y. Endo, A. Buckler-White, R. Plishka, N. Bischofberger, V. Hirsch, and M. A. Martin.** 2001. Macrophage are the principal reservoir and sustain high virus loads in rhesus macaques after the depletion of CD4$^+$ T cells by a highly pathogenic simian immunodeficiency virus/HIV type 1 chimera (SHIV): implications for HIV-1 infections of humans. Proc. Natl. Acad. Sci. USA **98:**658–663.
8. **Igarashi, T., O. K. Donau, H. Imamichi, M. J. Dumaurier, R. Sadjadpour, R. J. Plishka, A. Buckler-White, C. Buckler, A. F. Suffredini, H. C. Lane, J. P. Moore, and M. A. Martin.** 2003. Macrophage-tropic simian/human immunodeficiency virus chimeras use CXCR4, not CCR5, for infections of rhesus macaque peripheral blood mononuclear cells and alveolar macrophages. J. Virol. **77:**13042–13052.
9. **Ito, M., H. Hiramatsu, K. Kobayashi, K. Suzue, M. Kawahata, K. Hioki, Y. Ueyama, Y. Koyanagi, K. Sugamura, K. Tsuji, T. Heike, and T. Nakahata.** 2002. NOD/SCIDγ_c^{null} mouse: an excellent recipient mouse model for engraftment of human cells. Blood **100:**3175–3182.
10. **Kaneshima, H., L. Su, M. L. Bonyhadi, R. I. Connor, D. D. Ho, and J. M. McCune.** 1994. Rapid-high, syncytium-inducing isolates of human immunodeficiency virus type 1 induce cytopathicity in the human thymus of the SCID-hu mouse. J. Virol. **68:**8188–8192.
11. **Kollet, O., A. Peled, T. Byk, H. Ben-Hur, D. Greiner, L. Shultz, and T. Lapidot.** 2000. β2 Microglobulin-deficient (B2m^{null}) NOD/SCID mice are excellent recipients for studying human stem cell function. Blood **95:**3102–3105.
12. **Koot, M., I. P. Keet, A. H. Vos, R. E. de Goede, M. T. Roos, R. A. Coutinho, F. Miedema, P. T. Schellekens, and M. Tersmette.** 1993. Prognostic value of HIV-1 syncytium-inducing phenotype for rate of CD4$^+$ cell depletion and progression to AIDS. Ann. Intern. Med. **118:**681–688.
13. **Koyanagi, Y., Y. Tanaka, J. Kira, M. Ito, K. Hioki, N. Misawa, Y. Kawano, K. Yamasaki, R. Tanaka, Y. Suzuki, Y. Ueyama, E. Terada, T. Tanaka, M. Miyasaka, T. Kobayashi, Y. Kumazawa, and N. Yamamoto.** 1997. Primary human immunodeficiency virus type 1 viremia and central nervous system invasion in a novel hu-PBL-immunodeficient mouse strain. J. Virol. **71:**2417–2424.
14. **Matsumura, T., Y. Kametani, K. Ando, Y. Hirano, I. Katano, R. Ito, M. Shiina, H. Tsukamoto, Y. Saito, Y. Tokuda, S. Kato, M. Ito, K. Motoyoshi, and S. Habu.** 2003. Functional CD5$^+$ B cells develop predominantly in the spleen of NOD/SCID/γc^{null} (NOG) mice transplanted either with human umbilical cord blood, bone marrow, or mobilized peripheral blood CD34$^+$ cells. Exp. Hematol. **31:**789–797.
15. **McCune, J., H. Kaneshima, J. Krowka, R. Namikawa, H. Outzen, B. Peault, L. Rabin, C. C. Shih, E. Yee, M. Lieberman, I. Weissman, and L. Shultz.** 1991. The SCID-hu mouse: a small animal model for HIV infection and pathogenesis. Annu. Rev. Immunol. **9:**399–429.
16. **Mosier, D. E., R. J. Gulizia, S. M. Baird, D. B. Wilson, D. H. Spector, and S. A. Spector.** 1991. Human immunodeficiency virus infection of human-PBL-SCID mice. Science **251:**791–794.
17. **Mosier, D. E., R. J. Gulizia, P. D. MacIsaac, B. E. Torbett, and J. A. Levy.** 1993. Rapid loss of CD4$^+$ T cells in human-PBL-SCID mice by noncytopathic HIV isolates. Science **260:**689–692.
18. **Namikawa, R., H. Kaneshima, M. Lieberman, I. L. Weissman, and J. M. McCune.** 1988. Infection of the SCID-hu mouse by HIV-1. Science **242:**1684–1686.
19. **Shultz, L. D., P. A. Schweitzer, S. W. Christianson, B. Gott, I. B. Schweitzer, B. Tennent, S. McKenna, L. Mobraaten, T. V. Rajan, D. L. Greiner, et al.** 1995. Multiple defects in innate and adaptive immunologic function in NOD/LtSz-scid mice. J. Immunol. **154:**180–191.
20. **Tersmette, M., R. A. Gruters, F. de Wolf, R. E. de Goede, J. M. Lange, P. T. Schellekens, J. Goudsmit, H. G. Huisman, and F. Miedema.** 1989. Evidence for a role of virulent human immunodeficiency virus (HIV) variants in the pathogenesis of acquired immunodeficiency syndrome: studies on sequential HIV isolates. J. Virol. **63:**2118–2125.
21. **Ueda, T., H. Yoshino, K. Kobayashi, M. Kawahata, Y. Ebihara, M. Ito, S. Asano, T. Nakahata, and K. Tsuji.** 2000. Hematopoietic repopulating ability of cord blood CD34$^+$ cells in NOD/Shi-*scid* mice. Stem Cells **18:**204–213.
22. **Watanabe, S., K. Terashima, S. Ohta, S. Horibata, M. Yajima, Y. Shiozawa, M. Z. Dewan, Z. Yu, M. Ito, T. Morio, N. Shimizu, M. Honda, and N. Yamamoto.** 2007. Hematopoietic stem cell-engrafted NOD/SCID/IL2Rγ^{null} mice develop human lymphoid systems and induce long-lasting HIV-1 infection with specific humoral immune responses. Blood **109:**212–218.
23. **Yahata, T., K. Ando, Y. Nakamura, Y. Ueyama, K. Shimamura, N. Tamaoki, S. Kato, and T. Hotta.** 2002. Functional human T lymphocyte development from cord blood CD34$^+$ cells in nonobese diabetic/Shi-*scid*, IL-2 receptor γ null mice. J. Immunol. **169:**204–209.
24. **Zhang, L., G. I. Kovalev, and L. Su.** 2007. HIV-1 infection and pathogenesis in a novel humanized mouse model. Blood **109:**2978–2981.

Inhibiting lentiviral replication by HEXIM1, a cellular negative regulator of the CDK9/cyclin T complex

Saki Shimizu[a,b], Emiko Urano[a], Yuko Futahashi[a], Kosuke Miyauchi[a], Maya Isogai[a], Zene Matsuda[a], Kyoko Nohtomi[a], Toshinari Onogi[a], Yutaka Takebe[a], Naoki Yamamoto[a,b] and Jun Komano[a]

Objective: Tat-dependent transcriptional elongation is crucial for the replication of HIV-1 and depends on positive transcription elongation factor b complex (P-TEFb), composed of cyclin dependent kinase 9 (CDK9) and cyclin T. Hexamethylene bisacetamide-induced protein 1 (HEXIM1) inhibits P-TEFb in cooperation with 7SK RNA, but direct evidence that this inhibition limits the replication of HIV-1 has been lacking. In the present study we examined whether the expression of FLAG-tagged HEXIM1 (HEXIM1-f) affected lentiviral replication in human T cell lines.

Methods: HEXIM1-f was introduced to five human T cell lines, relevant host for HIV-1, by murine leukemia virus vector and cells expressing HEXIM1-f were collected by fluorescence activated cell sorter. The lentiviral replication kinetics in HEXIM1-f-expressing cells was compared with that in green fluorescent protein (GFP)-expressing cells.

Results: HIV-1 and simian immunodeficiency virus replicated less efficiently in HEXIM1-f-expressing cells than in GFP-expressing cells of the five T cell lines tested. The viral revertants were not immediately selected in culture. In contrast, the replication of vaccinia virus, adenovirus, and herpes simplex virus type 1 was not limited. The quantitative PCR analyses revealed that the early phase of viral life cycle was not blocked by HEXIM1. On the other hand, *Tat*-dependent transcription in HEXIM1-f-expressing cells was substantially repressed as compared with that in GFP-expressing cells.

Conclusion: These data indicate that HEXIM1 is a host factor that negatively regulates lentiviral replication specifically. Elucidating the regulatory mechanism of HEXIM1 might lead to ways to control lentiviral replication.

AIDS 2007, **21**:575–582

Keywords: CDK9, cyclin T, HEXIM1, lentivirus, *tat*

Introduction

Activation of transcription elongation requires the positive transcription elongation factor b complex (P-TEFb) composed of cyclin dependent kinase 9 (CDK9) and cyclin T1, T2, or K [1]. P-TEFb is essential for efficient transcriptional elongation from the promoter of human immunodeficiency virus type 1 (HIV-1), the long terminal repeat (LTR) (reviewed in [2,3]). The functional interaction between P-TEFb and the viral protein Tat has been well studied. Immediately after viral transcription starts at the LTR of the integrated proviral genome, the nascent viral transcript forms a three-dimensional structure called TAR. In the presence of P-TEFb, Tat binds to TAR. Through the Tat–TAR interaction, Tat activates P-TEFb and therefore assures the efficient

From the [a]AIDS Research Center, National Institute of Infectious Diseases, Tokyo, and the [b]Department of Molecular Virology, Tokyo Medical and Dental University, Tokyo, Japan.

Correspondence to Jun Komano, AIDS Research Center, National Institute of Infectious Diseases, 1-23-1 Toyama, Shinjuku, Tokyo 162-8640, Japan.

E-mail: ajkomano@nih.go.jp

Received: 9 July 2006; revised: 25 October 2006; accepted: 13 November 2006.

ISSN 0269-9370 © 2007 Lippincott Williams & Wilkins

completion of viral gene transcription and the propagation of HIV-1.

Recently, the regulatory mechanisms of P-TEFb function have been elucidated. In 2001, the interaction of P-TEFb with 7SK RNA was found to be necessary to inactivate the kinase activity of CDK9 within P-TEFb [4–6]. However, the binding of 7SK RNA alone is not sufficient to inactivate P-TEFb. More recently, Yik *et al.* demonstrated that the inactivation of P-TEFb requires hexamethylene bisacetamide-induced protein 1 (HEXIM1; synonyms CLP1, MAQ1, and HIS1) [7–9]. The inactivation of P-TEFb by the HEXIM1-7SK RNA complex appears to regulate the transcriptional elongation of cellular genes.

The HEXIM1-7SK RNA complex has been shown to physically compete with Tat for binding to P-TEFb [10]. In agreement with this finding, HEXIM1 was shown to inhibit Tat-dependent transcription from the HIV-1 LTR in transient transfection assays [8,11,12]. However, no data demonstrating that HEXIM1 is able to limit HIV-1 replication has been provided. Here we provide direct experimental evidence that the constitutive expression of HEXIM1 specifically limits lentiviral replication.

Methods

Plasmids

The FLAG-tagged HEXIM1 expression constructs were generated by reverse-transcription PCR using RNA isolated from CEM cells as templates. The primers used were 5′-CACCTCGAGCCACCATGGACTACAAAGACGATGACGACAAGGCCGAGCCATTCTTGTC-3′ and 5′-CAATTGCTAGTCTCCAAACTTGGAAAGCGGCGC-3′′ for amino terminus FLAG tagging, and 5′-CACCTCGAGCCACCATGGCCGAGCCATTCTTGTCAGAATATC-3′ and 5′-CAATTGCTAGTCGTCATCGTCTTTGTAGTCGTCTCCAAACTTGGAAAGCGGCGCTC-3′ for carboxy terminus FLAG tagging. The *Xho*I-*Mfe*I fragments of the PCR products were cloned into the *Xho*I-*Mfe*I sites of pCMMP IRES GFP, generating pCMMP f-HEXIM1 and pCMMP HEXIM1-f [13]. The cytomegalovirus (CMV) promoter-driven *gag-pol* expression vector psyn*gag-pol* has been previously described by Wagner *et al.* [14] and pLTR*gag-pol* was constructed by cloning the *Mlu*I-*Hin*dIII fragment encoding the LTR from pNL-luc [15] into the *Mlu*I-*Hin*dIII sites of psyn*gag-pol*. The tax expressing plasmid pCGtax and pHTLV LTR luciferase were kindly provided by Dr. Watanabe (Tokyo Medical Institute). The *tat*-expressing plasmid pSVtat was a generous gift from Dr. Freed (National Cancer Institute-Frederick, Frederick, Maryland, USA). The plasmid pLTR-luc has been described previously (Miyauchi *et al.*, *Antiviral Chemistry and Chemotherapy*, in press). The following plasmids have been described previously by Komano *et al.* [13]: pVSV-G, pMD*gag-pol*, pTM3Luci, phRL-CMV and pSIVmac239ΔnefLuc.

Cells and transfection

All the mammalian cells were maintained in RPMI 1640 (Sigma, St Louis, Missouri, USA) supplemented with 10% fetal bovine serum (Japan Bioserum, Tokyo, Japan), penicillin and streptomycin (Invitrogen, Tokyo, Japan). Cells were incubated at 37°C in a humidified 5% CO_2 atmosphere. Cells were transfected using Lipofectamine 2000 according to the manufacturer's protocol (Invitrogen).

Western blotting

Cells were lysed with sample buffer, sonicated, and boiled for 5 min. Samples were separated on 8% sodium dodecyl sulfate-polyacrylamide gel electrophoresis gels and transferred to polyvinylidene difluoride membranes (Millipore, Billerica, Massachusetts, USA) for western blotting according to standard techniques. Membranes were blocked with Tris-buffered saline containing 0.05% Tween-20 (TBS-T) containing 5% (w/v) non-fat skim milk (Yuki-Jirushi, Tokyo, Japan) for 1 h at room temperature and incubated with primary antibodies including the M2 anti-FLAG epitope monoclonal antibody (Sigma), an anti-actin monoclonal antibody (MAB1501R; Chemicon/Millipore, Billerica, Massachusetts, USA), an anti-cyclin T1 rabbit polyclonal antibody (H-245; Santa Cruz Biotechnology, Santa Cruz, California, USA), an anti-cyclin T2a/b goat polyclonal antibody (A-20; Santa Cruz), an anti-p24 monoclonal antibody (183-H12-5C; NIH AIDS Research and Reference Reagent Program), an anti-HIS1 chicken polyclonal antibody (N-150; GenWay, San Diego, California, USA), and an anti-Bip/GRP78 monoclonal antibody (clone 40; BD Biosciences/Transduction Laboratories, San Jose, California, USA) for 1 h at room temperature. Membranes were washed with TBS-T and incubated with appropriate second antibodies including biotinylated anti-goat (GE Healthcare Bio-Sciences, Piscataway, New Jersey, USA) or anti-chicken IgY (Promega, Madison, Wisconsin, USA), and EnVision+ (Dako, Glostrup, Denmark) for 1 h at room temperature. For a tertiary probe, we used horseradish peroxidase (HRP)-streptavidine (GE Healthcare) if necessary. Signals were visualized with an LAS3000 imager (Fujifilm, Tokyo, Japan) after treating the membranes with the Lumi-Light Western Blotting Substrate (Roche Diagnostics GmbH, Mannheim, Germany).

Reporter assay

Luciferase activity was measured 48 h after transfection or infection using a DualGlo assay kit (Promega) according to the manufacturer's protocol. The beta-galactosidase activity was measured using a LumiGal assay kit (BD Biosciences/Clontech, San Jose, California, USA) according to the manufacturer's protocol. The

chemiluminescence was detected with a Veritas luminometer (Promega).

Monitoring viral replication

To monitor HIV-1 replication, the culture supernantants were subjected to either a reverse transcriptase assay [16] or an enzyme-linked immunosorbent assay (ELISA) to detect p24 antigens using a Retro TEK p24 antigen ELISA kit according to the manufacturer's protocol (Zepto Metrix, Buffalo, New York, USA). For simian immunodeficiency virus (SIV) a p27 antigen ELISA kit was used according to the manufacturer's protocol (Zepto Metrix). The signals were measured with a Multiskan Ex microplate photometer (ThermoLabsystems, Helsinki, Finland). For vaccinia virus, adenovirus, and herpes simplex virus (HSV)-1, the activity of reporter genes was measured as previously described [13].

Generating viruses

To produce HIV-1 and SIV, 293T cells were transfected with plasmids encoding proviral DNA of HIV-1 (pHXB2) or pSIVmac239ΔnefLuc and culture supernatants containing viruses were collected at 48 h post-transfection. Murine leukemia virus (MLV) and lentiviral vectors pseudotyped with VSV-G were produced as described previously by cotransfecting 293T cells with either the pNL-Luc and pVSV-G vectors or the pMD*gag-pol*, pVSV-G, and pCMMP vectors [13]. Green fluorescent cells were sorted by fluorescence activated cell sorter (FACS) Aria (Becton Dickinson, San Jose, California, USA).

Reverse transcriptase-polymerase chain reaction

Total RNA was isolated with an RNeasy kit (Qiagen GmbH, Hilden, Germany) according to the manufacturer's instruction. The reverse transcriptase (RT)-polymerase chain reaction (PCR) assay was performed with a One Step RNA PCR Kit (Takara, Otsu, Japan), imaged by a Typhoon scanner 9400 (GE Healthcare), and quantified with Image Quant software (GE Healthcare). For the amplification of endogenous HEXIM1, the forward primer 5′-ACCACACGGAGAGCCTGCAGAAC-3′ and the reverse primer 5′-TAGCTAAATTTACGAAACCAAAGCC-3′ were used. For the amplification of HEXIM1-f, the forward primer 5′-GTACCTGGAACTGGAGAAGTGCCC-3′ and the reverse primer 5′-CAATTGCTAGTCGTCATCGTCTTTGTAGTC-3′ were used. For cyclophilin A, the forward primer 5′-CACCGCCACCATGGTCAACCCCACCGTGTTCTTCGAC-3′ and the reverse primer 5′-CCCGGGCCTCGAGCTTTCGAGTTGTCCACAGTCAGCAATGG-3′ were used.

Quantitative real time polymerase chain reaction

The real time PCR reaction was performed in a DNA Engine Opticon 2 Continuous Fluorescence Detection System (Bio-Rad, Hercules, California, USA). The cellular genomic DNA and total RNA were extracted 48 h post-infection with a DNeasy kit (Qiagen) and RNeasy kit (Qiagen), respectively, according to the manufacturer's instruction. For the reagents, we used QuantiTect SYBR Green PCR and RT-PCR Kits (Qiagen). To estimate the amount of integrated HIV-1 DNA, Alu-LTR PCR was performed according to the method described previously using the following primers: for the first PCR, 5′-AACTAGGGAACCCACTGCTTAAG-3′ and 5′-TGCTGGGATTACAGGCGTGAG-3′, and for the second PCR, 5′-AACTAGGGAACCCACTGCTTAAG-3′ and 5′-CTGCTAGAGATTTTCCACACTGAC-3′ [17]. The beta-globin primers have been described previously [18]. To estimate the amount of HIV-1 RNA, the second PCR primers for the Alu-LTR PCR were used. The primers for cyclophilin A are described above.

Results and discussion

The HEXIM1 cDNA tagged with a FLAG epitope at either the amino terminus (f-HEXIM1) or the carboxy terminus (HEXIM1-f) was cloned in a mammalian expression plasmid (Fig. 1a). A luciferase assay revealed that the Tat-dependent enhancement of transcription from the HIV-1 LTR was reduced by co-transfecting HEXIM1-expressing plasmids, whereas neither Tat-independent basal transcription from the HIV-1 LTR nor CMV promoter-driven transcription was affected (Fig. 1b). An oncogenic retrovirus human T cell leukemia virus type 1 (HTLV-1) encodes for *tax*, a functional homologue of HIV-1's *tat*, that utilizes P-TEFb to enhance transcription from the LTR promoter [19]. However, *tax*-dependent enhancement of transcription was not affected by HEXIM1 in similar experimental conditions (Fig. 1c). To monitor the effect of HEXIM1 on HIV-1 replication, we introduced HEXIM1-expressing plasmids into HeLa-CD4 cells along with pNL4-3, which produces replication-competent HIV-1, and measured the RT activity in the culture supernatant 1 week post-transfection. Transfecting HEXIM1-expressing plasmids decreased the RT activity in a dose-dependent manner (Fig. 1d). Next, we asked whether the inhibition of viral replication was specific to HIV-1 by examining vaccinia virus, adenovirus, and HSV-1 replication. We found that the propagation of these three viruses was not inhibited by HEXIM1-f expression (Fig. 1e–g), suggesting that the inhibition of viral replication by HEXIM1 was HIV-1-specific.

To examine whether HEXIM1 negatively affects lentiviral replication in the physiologically relevant host, we isolated human T cell lines constitutively expressing HEXIM1-f. We cloned HEXIM1-f cDNA into a pCMMP (MLV retroviral vector plasmid (Fig. 2a). The plasmid encoded an internal ribosomal entry site (IRES)-mediated green fluorescent protein (GFP) expression cassette, so that MLV vector-infected cells

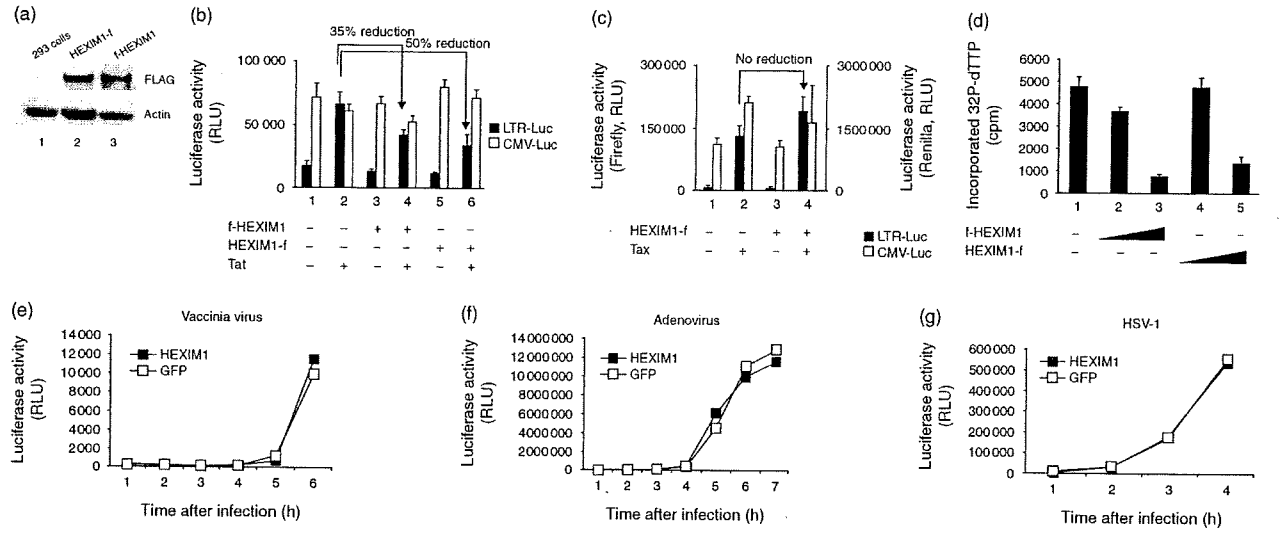

Fig. 1. Expression of hexamethylene bisacetamide-induced protein 1 (HEXIM1) specifically inhibits HIV-1 replication. (a) Detection of HEXIM1 cDNA tagged with a FLAG epitope at either the amino terminus (f-HEXIM1) or the carboxy terminus (HEXIM1-f) by western blot analysis in transiently transfected 293 cells (upper panel, approximately 65 kD). A western blot against actin is shown as a loading control (lower panel). (b) Expressing FLAG-tagged HEXIM1 decreased the luciferase activity driven by HIV-1 long terminal repeat (LTR) promoter in the presence of Tat (lanes 4 and 6, LTR-Luc, solid bars). However, FLAG-tagged HEXIM1 did not affect the expression of renilla luciferase from co-transfected plasmid driven by the cytomegalovirus (CMV) promoter (CMV-Luc, open bars). Representative data from three independent experiments done in triplicate are shown. Cells were transfected with 0.8 μg HEXIM1-expressing plasmid for the indicated lanes, 0.1 μg of pSV*tat* for the indicated lanes, and 0.1 μg of pLTR-Luc and 0.5 μg for phRL/CMV for all lanes. (c) Expressing FLAG-tagged HEXIM1 did not decrease the luciferase activity driven by HTLV-1 LTR promoter in the presence of Tax (lanes 2 and 4, LTR-Luc, solid bars) as well as renilla luciferase driven by the CMV promoter (CMV-Luc, open bars). Representative data from three independent experiments done in triplicate are shown. Cells were transfected with 0.8 μg of HEXIM1-expressing plasmid for the indicated lanes, 0.1 μg of pCGtax for the indicated lanes, and 0.1 μg of pHTLV LTR Luc and 0.5 μg for phRL/CMV for all lanes. (d) The dose-dependent reduction of HIV-1 production by transfection of HEXIM1-encoding plasmids (0.1 μg for lanes 2 and 4, 0.4 μg for lanes 3 and 5) along with a plasmid producing infectious HIV-1 (pNL4-3, 0.1 μg) in HeLa-CD4 cells. (e–g) Expressing HEXIM1-f did not limit the replication of vaccinia virus (e), adenovirus (f), or HSV-1 (g) in 293T cells. The *y*-axis represents the reporter gene activity, which reflects viral replication. Representative data from three independent experiments are shown. GFP, green fluorescent protein; RLU, relative light unit.

could be readily identified by the green fluorescence. Human T cell lines, including SUP-T1, MOLT-4, CEM, Jurkat, and M8166 were infected with MLV pseudotyped with vesicular stomatitis virus glycoprotein (VSV-G), and GFP-positive cells were collected with a FACS (Fig. 2a). For the negative control, we used MLV expressing GFP only. The successful introduction of HEXIM1-f into the cells was verified by RT-PCR and Western blot analysis (Fig. 2b and c). The total HEXIM1 protein expression in HEXIM1-f-transduced cells was approximately 3.7-, 1.5-, 2.0-, 4.8-, and 1.8-fold higher than in GFP-transduced cells in the CEM, Jurkat, MOLT-4, SUP-T1, and M8166 cell lines, respectively (Fig. 2c). To our surprise, the HEXIM1-f-expressing T cell lines remained GFP-positive, and therefore HEXIM1-f-positive, for more than 6 months and proliferated at rates almost indistinguishable from GFP-expressing cells. The expression levels of cyclin T1, cyclin T2, actin, and Bip/GRK78 in HEXIM1-f-expressing cells were almost identical to those in GFP-expressing cells, suggesting that the gene expression did not compensate the upregulated HEXIM1 (Fig. 2b and c). Expression of cyclin T2 was undetectable in M8166 cells (Fig. 2c). Similarly, HEXIM1-f expression did not affect the cell surface levels of the HIV-1 receptors CD4 and CXCR4 as demonstrated by FACS analysis (data not shown). These data indicate that the expression of HEXIM1-f did not reach levels where the physiological regulation of P-TEFb blocked cellular gene transcription.

The replication kinetics of HIV-1 or SIV was monitored by measuring the accumulation of viral capsid antigen in the culture medium. Strikingly, HIV-1 replicated more slowly in cells of all four T cell lines expressing HEXIM1-f than in cells expressing GFP (Fig. 2d–g). Similarly, HEXIM1-f-expressing M8166 cells supported SIV replication less efficiently than did GFP-expressing M8166 cells (Fig. 2h). Interestingly, the magnitude of HIV-1 replication delay was the most substantial in SUP-T1 cells, in which the levels of endogenous HEXIM1 were the lowest among the four cell lines tested for HIV-1 replication (Fig. 2c). Similar observations were made when the HIV-1 infection experiments were repeated, indicating that the expression of functional HEXIM1-f did not change over the course of the replication monitoring. We tested whether the viruses emerged in

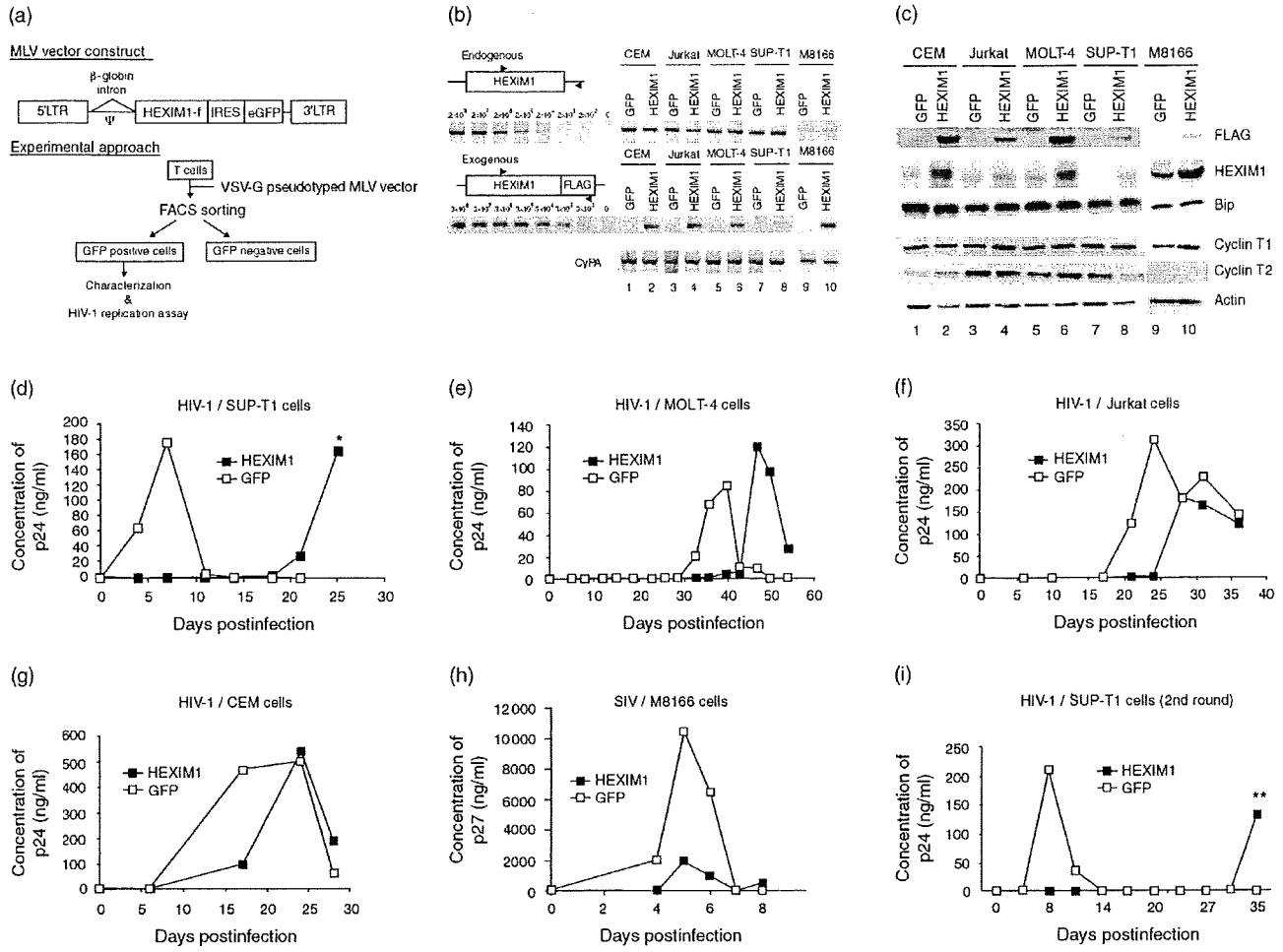

Fig. 2. Lentiviral replication is inhibited in various T cell lines constitutively expressing hexamethylene bisacetamide-induced protein 1 (HEXIM-1) cDNA tagged with a FLAG epitope at the carboxy terminus (HEXIM1-f). (a) The genomic organization of the retroviral vector expressing HEXIM1-f and a schematic representation of the experimental approach. (b) Detection of endogenous HEXIM1 and murine leukemia virus (MLV)-transduced HEXIM1-f (exogenous) mRNA by reverse transcriptase-polymerase chain reaction in green fluorescent protein (GFP)- and HEXIM1-f-expressing cells. The primer design is drawn schematically. Amplification efficiency was examined by using a known number of templates as standards for HEXIM1. Cyclophilin A (CyPA) was amplified to ensure the quality of the RNA. (c) Western blot analysis demonstrating expression of HEXIM1-f (denoted FLAG), endogenous HEXIM1 (HEXIM1), Bip, cyclin T1, cyclin T2, and actin in isolated T cell lines. (d–g) Replication profiles of HIV-1 (HXB2) in SUP-T1 (d), MOLT-4 (e), Jurkat (f), and CEM (g) cells either expressing HEXIM1-f or GFP alone. Representative data from two or three independent experiments are shown. (h) Replication profile of SIV in M8166 cells either expressing HEXIM1-f or GFP alone. Representative data from two independent experiments are shown. (i) The replication profiles of HIV-1 recovered from SUP-T1/HEXIM1-f cells (asterisk in Fig. 2d) in fresh SUP-T1/GFP or SUP-T1/HEXIM1-f. LTR, long terminal repeat.

HEXIM1-f-expressing cells were 'revertants' that might be able to replicate in HEXIM1-f-expressing cells as fast as in GFP-expressing cells. To address this, we recovered virus-containing culture supernatants from SUP-T1/HEXIM1-f cells at the peak of replication kinetics (asterisk, Fig. 2d). Then, both fresh SUP-T1/GFP and SUP-T1/HEXIM1-f were infected with the recovered virus and the replication kinetics was monitored. However, HIV-1 still replicated in SUP-T1/HEXIM1-f cells more slowly than in SUP-T1/GFP cells (Fig. 2i), akin to the original profiles (Fig. 2d), and the nucleotide sequences of LTR and *tat*, the primary targets of HEXIM1, remained unchanged (double asterisk in Fig. 2i). In addition, no mutations were found in viruses propagated in GFP-expressing SUP-T1 cells. Similar observations were made in MOLT-4 cells (data not shown). These data provide direct evidence that the expression of HEXIM1 inhibits lentiviral replication in human T cell lines.

Based on our experimental observations as well as the reported functions of HEXIM1, we assumed that the ability of HEXIM1 to limit HIV-1 replication was mostly due to the inhibition of Tat/P-TEFb-dependent transcriptional elongation. However, it was possible that HEXIM1 might also have targeted other viral replication

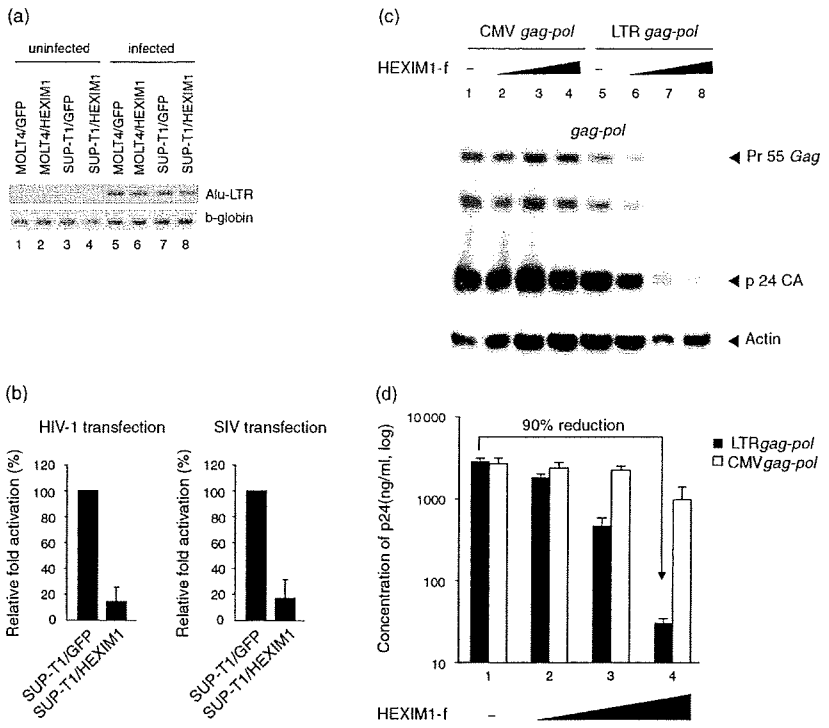

Fig. 3. Hexamethylene bisacetamide-induced protein 1 (HEXIM1) cDNA tagged with a FLAG epitope at the carboxy terminus (HEXIM1-f) does not affect the efficiency of viral integration or post-translational processes. (a) The Alu-long terminal repeat (LTR) and beta-globin polymerase chain reaction products from VSV-G-pseudotyped HIV-1-infected MOLT-4 and SUP-T1 cells expressing either green fluorescent protein (GFP) or HEXIM1-f alone were separated in an agarose gel and photographed. (b) The luciferase activities in SUP-T1/GFP or SUP-T1/HEXIM1-f cells electroporated with 10 μg of a plasmid encoding LTR-driven firefly luciferase plus 1 μg of phRL/cytomegalovirus (CMV). The firefly luciferase activity normalized to renilla luciferase activity in SUP-T1/GFP cells was set to 100%. The error bars represent the standard deviation of three independent experiments. (c) Western blot analysis showing Gag and its cleaved products expressed from either CMV promoter- or LTR promoter-driven *gag-pol* expression plasmid in the presence of pSVtat (0.1 μg, all lanes) and increasing amounts of HEXIM1-f (0.2 μg for lanes 2 and 6, 0.6 μg for lanes 3 and 7, and 2.0 μg for lanes 4 and 8). (d) The amount of p24 produced in the culture supernatant from cells analyzed in Fig. 3c was measured by enzyme-linked immunosorbent assay. Representative data from three independent experiments done in triplicate are shown. SIV, simian immunodeficiency virus.

steps. To test this possibility, we examined the viral entry and production processes separately. The efficiency of viral entry was analyzed by measuring the efficiency of viral integration. SUP-T1/GFP or SUP-T1/HEXIM1-f cells were infected with a replication-incompetent HIV-1 vector pseudotyped with VSV-G that expresses luciferase upon successful infection. We conducted an Alu-LTR PCR assay to detect the integrated viral genome. PCR products were detected only from HIV-1-infected cells (Fig. 3a). The signal intensities of Alu-LTR PCR products from GFP- and HEXIM1-f-experssing cells were similar. To compare the efficiency of viral infection as well as transcription quantitatively, we employed a real time PCR technique. Some infected cells were collected for an Alu-LTR PCR assay to quantify the amount of integrated viral genome, and the rest were processed to measure the amount of viral transcript as well as the luciferase activity. The amount of Alu-LTR PCR product from SUP-T1/HEXIM1-f cells was 3.5- and 3.3-fold more to that from SUP-T1/GFP cells from two independent experiments, respectively (Table 1). These data suggest that the efficiency of viral integration was not inhibited in HEXIM1-f-expressing SUP-T1 cells. In contrast, the relative abundance of HIV-1 transcript expressed in SUP-T1/HEXIM1-f cells was substantially decreased to 0.03 and 2.9% relative to SUPT1/GFP cells (Table 1). Furthermore, the luciferase activities were 200-fold lower in SUP-T1/HEXIM1-f cells than in SUP-T1/GFP cells (Table 1). Similar data was obtained from MOLT-4 cells infected with HIV-1 pseudotyped with VSV-G (data not shown). The transfection of plasmids encoding reporter viral DNA can bypass the viral entry and make it possible to measure the effect of HEXIM1 on LTR-driven transcription and translation. Consistent with above data, transfecting pNL-Luc into SUP-T1/HEXIM1-f cells gave significantly lower luciferase activities than SUP-T1/GFP cells (Fig. 3b, left). Similar data were obtained using pSIVmac239ΔnefLuc (Fig. 3b, right). These data strengthen the possibility that HEXIM1 targets post-integration processes.

Table 1. Effect of hexamethylene bisacetamide-induced protein 1 (HEXIM1) cDNA tagged with a FLAG epitope at the carboxy terminus (HEXIM1-f) on viral entry and transcription in SUP-T1 cells examined by quantitative real time polymerase chain reaction.

		Integrated HIV-1 genome			HIV-1 transcript			Luciferase activity	
Exp.	Transduced gene	Alu-LTR (copy)	β-globin (copy)	Normalized[a] (%)	HIV-1 RNA (copy)	CyPA (copy)	Normalized[b] (%)	RLU[c]	Normalized[d] (%)
1	GFP	5.2×10^5	6.7×10^6	100.0	1.6×10^6	6.8×10^7	100.0	3.2×10^5	100.0
	HEXIM1-f	2.0×10^6	7.4×10^6	351.3	6.7×10^1	1.0×10^8	0.03	1.5×10^3	0.5
2	GFP	4.6×10^6	1.8×10^7	100.0	3.1×10^8	8.9×10^7	100.0	7.1×10^5	100.0
	HEXIM1-f	1.6×10^7	1.9×10^7	333.2	9.4×10^6	9.3×10^7	2.9	3.4×10^3	0.5

[a]The number of Alu-long terminal repeat (LTR) products divided by the number of beta-globin products in SUP-T1/GFP is set to 100%. The abundance of Alu-LTR products in SUP-T1/HEXIM1-f relative to SUP-T1/green fluorescent protein (GFP) is shown.
[b]The number of HIV-1 RNA transcripts in SUP-T1/GFP divided by the number of cyclophilin A (CyPA) transcripts is set to 100%. The abundance of HIV-1 RNA in SUP-T1/HEXIM1-f relative to SUP-T1/GFP is shown.
[c]The luciferase activity is shown by relative light unit (RLU).
[d]The luciferase activity in SUP-T1/GFP is set to 100%. The luciferase activity in SUP-T1/HEXIM1-f relative to SUP-T1/GFP is shown.

To test this further, we analyzed the efficiency of post-transcriptional processes with a transient transfection assay measuring the amount of Pr55 Gag, a viral gene product, and virus-like particles (VLPs) produced in the culture supernatants. For this purpose, we used the CMV promoter-driven *gag-pol* expression plasmid, because HEXIM1-f did not affect CMV-driven transcription (Fig. 1b). At the levels of HEXIM1-f where LTR-driven Tat-dependent transcription was drastically inhibited (Fig. 3c, lanes 7, 8), the amount of CMV promoter-driven Gag expression was almost identical to that in the absence of HEXIM1-f (Fig. 3c, lanes 1–4). Furthermore, the processing pattern of Pr55 Gag in the presence of HEXIM1-f was identical to that in its absence (Fig. 3c). These data indicate that HEXIM1-f did not inhibit the transcription from a Tat-independent promoter, the translation of viral protein, or the protease activity of HIV-1. Finally, the potential effect of HEXIM1 on viral budding was examined. To do this, the amount of p24 CA in the culture supernatant of transfected cells was quantified as a representation of the amount of VLP. Expressing HEXIM1-f reduced VLP production from cells co-transfected with pLTR*gag-pol* and pSVtat at levels comparable to the protein expression levels (Fig. 3c and d). In contrast, expressing HEXIM1-f did not reduce the amount of VLP produced by cells co-transfected with pCMV*gag-pol* and pSVtat in conditions in which Tat-dependent LTR transcription was substantially inhibited (Fig. 3c and d). Taken together, this indicates that HEXIM1-f lowers the efficiency of Tat-dependent transcription from LTR promoter but does not block the efficiency of the late phase of the viral life cycle including translation, Gag's assembly, and budding. Thus, it is likely that HEXIM1 primarily targets Tat/P-TEFb-dependent transcription to inhibit HIV-1 replication.

Our findings demonstrated that HEXIM1, a cellular P-TEFb inhibitor, is a specific negative regulator of lentiviral replication in human T cell lines. The replication of vaccinia virus, adenovirus, and HSV-1 were not affected by HEXIM1-f expression; however, the *Tat*-dependent transcription of the LTR promoter of both HIV-1 and SIV was reduced by HEXIM1-f. HEXIM1 limited replication of HIV-1 dramatically at levels where it did not visibly affect cell physiology (as little as a 5-fold increase over the endogenous levels), nor were revertants immediately selected in HEXIM1-f-expressing cells. These data support the feasibility of developing HIV-1 inhibitors targeting the processes in which HEXIM1 is involved. For example, it is conceivable to hunt for a non-toxic chemical inducer for HEXIM1 since expression of HEXIM1 is induced by hexamethylene bisacetamide (HMBA) that is considerably toxic for cells [20].

P-TEFb has been shown to support transcription of the *c-myc* and CIITA transcription factors (reviewed in [21,22]). The functions of these transactivators are critical for cell proliferation, but in this study constitutive expression of HEXIM1-f, which reduces P-TEFb activity, did not affect the cell proliferation of human T cell lines, the human epithelial cell lines HEK293 or the NP2 glioblastoma cell lines (data not shown). How can this be explained? Very recently, a high-molecular-weight bromodomain protein, Brd4, was found to function as a 'cellular *tat*' [23,24]. Interestingly, it was shown that Brd4 binds not only to cyclin T1 but also to cyclin T2, a widely expressed variant of cyclin T, to which HEXIM1 binds but Tat does not [23–25]. We hypothesize that Brd4 might be able to recruit and activate P-TEFb more efficiently than does Tat, leaving cellular transcription unaffected by the upregulated expression of HEXIM1 from the retroviral vector. An alternative possibility comes from the fact that HEXIM1 does not interact with the ubiquitously expressed cyclin K, which functions as a P-TEFb component. It is possible that Tat is not able to utilize P-TEFb consisting of CDK9 and cyclin K but Brd4 can, such that cyclin K may substitute for cyclin T1 to support Brd4-mediated cellular gene transcription.

Acknowledgements

We thank Dr. Tsutomu Murakami for the critical reading of the manuscript. This work was partly supported by

Japan Health Science Foundation, Japanese Ministry of Health, Labor and Welfare, and Japanese Ministry of Education, Culture, Sports, Science and Technology.

Sponsorship: This work was partly supported by Japan Health Science Foundation, Japanese Ministry of Health, Labor and Welfare, and Japanese Ministry of Education, Culture, Sports, Science and Technology.

References

1. Marshall N, Price D. **Control of formation of two distinct classes of RNA polymerase II elongation complexes.** *Mol Cell Biol* 1992; **12**:2078–2090.
2. Kuiken C, Foley B, Hahn B, Korber B, Marx P, McCutchan F, *et al.*, editors. *HIV Sequence Compendium 2000.* Los Alamos: Theoretical Biology and Biophysics Group, Los Alamos National Laboratory, 2000.
3. Barboric M, Peterlin BM. **A new paradigm in eukaryotic biology: HIV Tat and the control of transcriptional elongation.** *PLoS Biol* 2005; **3**:e76.
4. Nguyen V, Kiss T, Michels A, Bensaude O. **7SK small nuclear RNA binds to and inhibits the activity of CDK9/cyclin T complexes.** *Nature* 2001; **414**:322–325.
5. Yang Z, Zhu Q, Luo K, Zhou Q. **The 7SK small nuclear RNA inhibits the CDK9/cyclin T1 kinase to control transcription.** *Nature* 2001; **414**:317–322.
6. Li Q, Price J, Byers S, Cheng D, Peng J, Price D. **Analysis of the large inactive P-TEFb complex indicates that it contains one 7SK molecule, a dimer of HEXIM1 or HEXIM2, and two P-TEFb molecules containing Cdk9 phosphorylated at threonine 186.** *J Biol Chem* 2005; **280**:28819–28826.
7. Michels A, Nguyen V, Fraldi A, Labas V, Edwards M, Bonnet F, *et al.* **MAQ1 and 7SK RNA interact with CDK9/cyclin T complexes in a transcription-dependent manner.** *Mol Cell Biol* 2003; **23**:4859–4869.
8. Yik J, Chen R, Pezda A, Samford C, Zhou Q. **A human immunodeficiency virus type 1 Tat-like arginine-rich RNA-binding domain is essential for HEXIM1 to inhibit RNA polymerase II transcription through 7SK snRNA-mediated inactivation of P-TEFb.** *Mol Cell Biol* 2004; **24**:5094–5105.
9. Barboric M, Kohoutek J, Price J, Blazek D, Price D, Peterlin B. **Interplay between 7SK snRNA and oppositely charged regions in HEXIM1 direct the inhibition of P-TEFb.** *EMBO J* 2005; **24**:4291–4303.
10. Schulte A, Czudnochowski N, Barboric M, Schonichen A, Blazek D, Peterlin B, Geyer M. **Identification of a cyclin T-binding domain in Hexim1 and biochemical analysis of its binding competition with HIV-1 Tat.** *J Biol Chem* 2005; **280**:24968–24977.
11. Fraldi A, Varrone F, Napolitano G, Michels A, Majello B, Bensaude O, Lania L. **Inhibition of Tat activity by the HEXIM1 protein.** *Retrovirology* 2005; **2**:42.
12. Michels A, Fraldi A, Li Q, Adamson T, Bonnet F, Nguyen V, *et al.* **Binding of the 7SK snRNA turns the HEXIM1 protein into a P-TEFb (CDK9/cyclin T) inhibitor.** *EMBO J* 2004; **23**:2608–2619.
13. Komano J, Miyauchi K, Matsuda Z, Yamamoto N. **Inhibiting the Arp2/3 complex limits infection of both intracellular mature vaccinia virus and primate lentiviruses.** *Mol Biol Cell* 2004; **15**:5197–5207.
14. Wagner R, Graf M, Bieler K, Wolf H, Grunwald T, Foley P, Uberla K. **Rev-independent expression of synthetic gag-pol genes of human immunodeficiency virus type 1 and simian immunodeficiency virus: implications for the safety of lentiviral vectors.** *Hum Gene Ther* 2000; **11**:2403–2413.
15. Masuda T, Planelles V, Krogstad P, Chen I. **Genetic analysis of human immunodeficiency virus type 1 integrase and the U3 att site: unusual phenotype of mutants in the zinc finger-like domain.** *J Virol* 1995; **69**:6687–6696.
16. Willey R, Smith D, Lasky L, Theodore T, Earl P, Moss B, *et al.* **In vitro mutagenesis identifies a region within the envelope gene of the human immunodeficiency virus that is critical for infectivity.** *J Virol* 1988; **62**:139–147.
17. Butler SL, Hansen MS, Bushman FD. **A quantitative assay for HIV DNA integration in vivo.** *Nat Med* 2001; **7**:631–634.
18. Graf Einsiedel H, Taube T, Hartmann R, Wellmann S, Seifert G, Henze G, Seeger K. **Deletion analysis of p16(INKa) and p15(INKb) in relapsed childhood acute lymphoblastic leukemia.** *Blood* 2002; **99**:4629–4631.
19. Zhou M, Lu H, Park H, Wilson-Chiru J, Linton R, Brady JN. **Tax interacts with P-TEFb in a novel manner to stimulate human T-lymphotropic virus type 1 transcription.** *J Virol* 2006; **80**: 4781–4791.
20. Kusuhara M, Nagasaki K, Kimura K, Maass N, Manabe T, Ishikawa S, *et al.* **Cloning of hexamethylene-bis-acetamide-inducible transcript, HEXIM1, in human vascular smooth muscle cells.** *Biomed Res* 1999; **20**:273–279.
21. Price DH. **P-TEFb, a cyclin-dependent kinase controlling elongation by RNA polymerase II.** *Mol Cell Biol* 2000; **20**:2629–2634.
22. Garriga J, Grana X. **Cellular control of gene expression by T-type cyclin/CDK9 complexes.** *Gene* 2004; **337**:15–23.
23. Jang M, Mochizuki K, Zhou M, Jeong H, Brady J, Ozato K. **The bromodomain protein Brd4 is a positive regulatory component of P-TEFb and stimulates RNA polymerase II-dependent transcription.** *Mol Cell* 2005; **19**:523–534.
24. Yang Z, Yik J, Chen R, He N, Jang M, Ozato K, Zhou Q. **Recruitment of P-TEFb for stimulation of transcriptional elongation by the bromodomain protein Brd4.** *Mol Cell* 2005; **19**:535–545.
25. Napolitano G, Licciardo P, Gallo P, Majello B, Giordano A, Lania L. **The CDK9-associated cyclins T1 and T2 exert opposite effects on HIV-1 Tat activity.** *AIDS* 1999; **13**:1453–1459.

Hematopoietic stem cell–engrafted NOD/SCID/IL2Rγ^{null} mice develop human lymphoid systems and induce long-lasting HIV-1 infection with specific humoral immune responses

Satoru Watanabe,[1] Kazuo Terashima,[2] Shinrai Ohta,[3] Shigeo Horibata,[3] Misako Yajima,[4] Yoko Shiozawa,[1] M. Zahidunnabi Dewan,[2,3] Zhong Yu,[2] Mamoru Ito,[5] Tomohiro Morio,[6] Norio Shimizu,[1] Mitsuo Honda,[3] and Naoki Yamamoto[2,3]

[1]Department of Virology, Division of Medical Science, Medical Research Institute, Tokyo Medical and Dental University, Japan; [2]Department of Molecular Virology, Graduate School of Medicine, Tokyo Medical and Dental University, Japan; [3]AIDS Research Center, National Institute of Infectious Diseases, Tokyo, Japan; [4]Department of Infectious Diseases, National Research Institute for Child Health and Development, Tokyo, Japan; [5]Central Institute for Experimental Animals, Kanagawa, Japan; and [6]Department of Pediatrics and Developmental Biology, Graduate School of Medicine, Tokyo Medical and Dental University, Japan

Critical to the development of an effective HIV/AIDS model is the production of an animal model that reproduces long-lasting active replication of HIV-1 followed by elicitation of virus-specific immune responses. In this study, we constructed humanized nonobese diabetic/severe combined immunodeficiency (NOD/SCID)/interleukin-2 receptor γ-chain knockout (IL2Rγ^{null}) (hNOG) mice by transplanting human cord blood–derived hematopoietic stem cells that eventually developed into human B cells, T cells, and other monocytes/macrophages and dendritic cells associated with the generation of lymphoid follicle–like structures in lymphoid tissues. Expressions of CXCR4 and CCR5 antigens were recognized on CD4$^+$ cells in peripheral blood, the spleen, and bone marrow, while CCR5 was not detected on thymic CD4$^+$ T cells. The hNOG mice showed marked, long-lasting viremia after infection with both CCR5- and CXCR4-tropic HIV-1 isolates for more than the 40 days examined, with R5 virus–infected animals showing high levels of HIV-DNA copies in the spleen and bone marrow, and X4 virus–infected animals showing high levels of HIV-DNA copies in the thymus and spleen. Furthermore, we detected both anti–HIV-1 Env gp120– and Gag p24–specific antibodies in animals showing a high rate of viral infection. Thus, the hNOG mice mirror human systemic HIV infection by developing specific antibodies, suggesting that they may have potential as an HIV/AIDS animal model for the study of HIV pathogenesis and immune responses. (Blood. 2007; 109:212-218)

Introduction

Current animal models for either human immunodeficiency virus type 1 (HIV-1) or simian immunodeficiency virus (SIV) suffer from the lack of a system precisely mirroring human HIV infection and the progression to disease state.[1] In current animal models with HIV infection, such as chimpanzees, animals do not develop AIDS.[1] Past animal models for HIV infection have relied on humanized severe combined immunodeficiency (hSCID) mice models to study prospective anti-HIV drugs and vaccines. SCID-hu (Thy/Liv) mice, engrafted with human fetal thymus and liver tissue in the renal subcapsular region, were first reported as the small-animal model.[2] Because human T cells are generated within the engrafted thymus, this model has been used for the study of thymopoiesis[3-6] and hematopoiesis[7,8] under the burden of HIV-1 infection. However, this model allows for a limited systemic HIV-1 infection, which is restricted mainly to the engrafted thymus. Another HIV mouse model, hu-PBL–SCID mice engrafted with human peripheral blood mononuclear cells (PBMCs),[9] has been actively used as a tool in developing antiretroviral therapy.[9-11] However, the infection persists for only a short time in association with rapid loss of CD4$^+$ T cells because there is no active hematopoiesis or thymopoiesis.[9,12,13] Furthermore, these mouse models fail to mirror certain key aspects of the human immune response, lacking normal lymphoid tissue and functional human antigen-presenting cells such as dendritic cells (DCs).[14] Thus, although these mouse models are valuable as animal models for HIV infection, the development of a mouse model more analogous to human HIV infection is needed if we are to better understand HIV pathogenesis and develop successful anti-HIV therapies and preventive vaccines.

To solve the difficult issue about the development of an ideal HIV mouse model, we initially selected a humanized nonobese diabetic (NOD)/SCID interleukin-2 receptor (IL-2R) γ-chain knockout (NOG) mouse[15] as a model animal because it has been suggested that multilineage cells, including human T, B, and natural killer (NK) cells, differentiate in these mice when given transplants of human CD34$^+$ hematopoietic stem cells.[16-18] In the current study, we further reveal the kinetics of differentiation of human B and T cells, monocytes/macrophages, and DCs in the mice that received transplants, and we characterize the animals by infection with both CCR5 (R5)– and CXCR4 (X4)-tropic HIV strains. Since our hNOG mice show stable and systemic infection of both R5- and X4-tropic HIV for more than

Submitted April 20, 2006; accepted August 12, 2006. Prepublished online as *Blood* First Edition Paper, September 5, 2006; DOI 10.1182/blood-2006-04-017681.

The publication costs of this article were defrayed in part by page charge payment. Therefore, and solely to indicate this fact, this article is hereby marked "advertisement" in accordance with 18 USC section 1734.